

A note on estimating the error when subtracting background counts from weak OSL signals

Bo Li

Department of Earth Sciences, The University of Hong Kong, Pokfulam Road, Hong Kong, China

(Received 15 March 2007; in final form 26 April 2007)

Abstract

The counting statistics of the instrumental background that underlies all OSL measurements was investigated and found not to follow a Poisson distribution. However, if the instrumental background is assumed to have a Poisson distribution, substantial underestimation of the error of the background-corrected OSL signal may occur, especially for samples with a weak OSL signal. An alternative method is suggested for estimating the error on the background-corrected OSL signal by making a separate measurement of the variance of the instrumental background.

Keywords: error, OSL, counting statistics, Poisson distribution

Introduction

Appropriate estimation of the error for the background-subtracted optically stimulated luminescence (OSL) signal is important for assessing the error of the age calculated in optical dating. The error in the OSL signal is commonly calculated by assuming a Poisson distribution (e.g. Galbraith et al., 1999). Based on this assumption, a formula for calculating the error in the background-corrected OSL signal was proposed by Banerjee et al. (2000). A correction of this formula and more detailed discussion related to the variance calculation for background-corrected OSL signals were given later by Galbraith (2002). In both reports, the OSL signal was assumed to consist of only two components, the initial OSL signal and a constant instrumental background. The error calculation formula was derived by assuming that both the OSL signal and the background follow a Poisson distribution. Although some cases where the background is over-dispersed have been discussed (Galbraith et al., 1999; Galbraith, 2002), the reasons for over-dispersion of the background are still not clear.

Several studies suggest that the OSL signal from quartz actually consists of several components, namely the fast, medium and slow components (e.g.

Smith and Rhodes, 1994; Bailey et al., 1997). In continuous-wave OSL (CW-OSL) measurement, the initial part of the signal that is commonly used for dating comes mainly from the fast component and some of the medium component, and the signal in the final part of the decay curve comes mainly from the slow component and the instrumental background (e.g. Li and Li, 2006); the latter is composed of the instrumental noise and scattered light. The slow component and instrumental background are considered to be constant throughout the optical stimulation and are estimated from the final part of the OSL curve. They are subtracted from the initial signal to obtain the background-corrected signal. Hence, the background described in Galbraith et al. (1999) is actually the sum of the instrumental background and the slow component.

Because the intensity of the slow component may vary from sample to sample, the relative contributions of the slow component and the instrumental background to the last part of the OSL signal also vary from sample to sample. Hence, simply assuming that the slow component and background have the same distribution may lead to incorrect estimation of the uncertainty. Thus the variances of the slow component and background observed in the final part of the OSL curve need to be considered separately and incorporated into the error calculation for the background-subtracted signal. This paper aims to investigate whether assuming that the instrumental background has a Poisson distribution is appropriate, and how this assumption would influence the error calculation.

Samples and analytical facilities

The OSL decay curves used in this study were obtained from the quartz extracts of several sediments from China, C5, Wgs1, TWC and DGF-1, used for optical dating. These samples have different initial OSL count rates, ranging from 10^2 to 10^5 cts/s. For OSL measurement, the mineral grains were mounted on 10-mm diameter and 0.5-mm thick aluminum discs with Silkospray silicone oil.

| | Disc Number | | | | | | Average |
|--|-------------|------|------|------|------|------|----------|
| | 1 | 2 | 3 | 4 | 5 | 6 | |
| Mean counts (counts/0.2s) | 12.9 | 12.9 | 12.8 | 12.7 | 13.6 | 12.9 | 13.0±0.1 |
| Variance (counts/0.2s) ² | 25.4 | 26.3 | 25.4 | 26.6 | 29.5 | 30.1 | 27.2±0.9 |
| Variance/Mean | 2.0 | 2.0 | 2.0 | 2.1 | 2.2 | 2.3 | 2.1±0.1 |

Table 1: The mean counts, variance and variance/ mean ratio of the instrumental background measurement of six aliquots with annealed quartz grains. The aliquots were measured under the same conditions as in OSL measurement (125°C for 100 s with 50% of the maximum power of the blue LEDs).

All measurements were performed using an automated Risø TL/OSL DA-15 reader equipped with excitation units containing blue light-emitting diodes (LEDs, 470 ± 30 nm) (Bøtter-Jensen et al., 1999). The OSL signal was detected by a photomultiplier tube (PMT) (EMI9235QA) observing the sample through 7.5 mm thickness of U-340 filters. All OSL measurements were carried out at 125°C using blue LEDs with 50% of the maximum power (~30 mW/cm²).

Results

Variability of the instrumental background

In order to test the variability of the background, some quartz grains extracted from these samples were annealed at 900°C for 2 hours to remove all the OSL signals. The grains were then mounted on six aluminum discs and optically stimulated using the same experimental conditions as those used in practical OSL measurements, i.e. the same stimulation light power and time, and the same holding temperature (125°C). The recording time per channel is the same as that used in OSL measurements (0.2s/channel in this paper). Because all the OSL signals have been removed by annealing, the observed counts should represent the instrumental background.

A typical background as a function of stimulation time from one of the aliquots (disc 6 in Table 1) is shown in Fig. 1. The background is independent of stimulation time with a mean count rate at 12.9 cts/0.2 s, and for the 500 channels shown the standard error is 0.2 cts/0.2 s. The variance is 30.1 (cts/0.2 s)² for the data set. A summary of the mean, variance and variance/mean ratio from the six aliquots, and the average of the values obtained are shown in Table 1. There is little difference of mean, variance and variance/mean ratio among the different aliquots, suggesting that the instrumental background and its distribution are similar under specified experimental conditions. The ratio of the variance/mean is 2.1 ± 0.1, rather than 1 as would be expected in the case of a Poisson distribution (e.g. Galbraith, 2002),

suggesting that the background is over-dispersed. It should be noted that the variance/mean ratio only changes negligibly if the total counts in successive n ($n > 1$) channels are analysed because the mean counts and the variance would increase proportionally with the integration time. For example, for 5 successive channels (integration time is 1 second), the mean count rate for the data set shown in Fig. 1 in 5 channels is 64 cts/s and the variance is 152 (cts/s)², which are all 5 times the values obtained when 1 channel was analysed (Table 1). The variance/mean is 2.4, similar to the value of 2.3 when successive channels (0.2 s) are analysed.

It should be remembered that in some instrumental systems there is electronic division of the signal by a factor of 2; this means that the true variance is 4 times the observed variance and the true count rate is twice the observed one. Therefore, in this case, the observed variance/mean ratio is actually underestimated by a factor of 2, although the relative standard error will not be affected. For this study, the true variance/mean ratio should thus be double the observed one, i.e. 4.2, which is still a strong indication of over-dispersion.

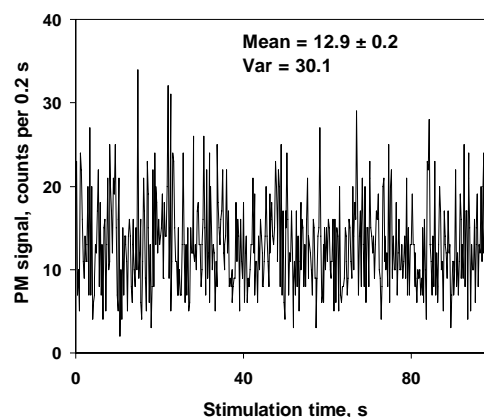


Figure 1: Typical background signal from annealed quartz grains mounted on an aluminum disc, which was measured under the same conditions as normal OSL measurements (125°C for 100 s with 50% of the maximum power of the blue LEDs).

In order to confirm that the measured counts as shown in Fig. 1 and Table 1 were purely from instrumental background, rather than from the possible residual signal of quartz grains, another six blank disks, prepared without mounting any grains, were measured under the same conditions as described above. A mean count rate of 12.7 ± 0.3 cts/0.2 s was obtained, indistinguishable from the value of 13.0 ± 0.1 cts/0.2 s when the grains were present (Table 1). This suggests that no signal came from the annealed quartz grains and there is little dependence of instrumental background on whether the quartz grains were mounted on the disks or not.

The fact that the variance/mean ratio is not 1 for the measurements without grains indicates that the instrumental background doesn't follow a Poisson distribution. Thus the error estimation based on the assumption that the background has a Poisson distribution will lead to underestimation of the true error. It is thus suggested that the instrumental background should be measured for each instrument to check whether it is appropriate to assume a Poisson distribution for the background for error calculation.

The formula for error estimation

Since the background doesn't follow a Poisson distribution, the variances of the slow component and background observed in the final part of an OSL curve need to be considered separately and incorporated into the error calculation for the background-subtracted signal. Using definitions similar to those used by Galbraith (2002), if Y_0 denotes the OSL signal observed in the initial stimulation time (or in the first n channels), by allowing for different OSL components, we have

$$Y_0 = S_{f+m} + S_{s0} + B_0 \quad \text{Eqn. 1}$$

where S_{f+m} is the fast and medium components in the first n channels, S_{s0} is the slow component and B_0 is the instrumental background in the first n channels. In CW-OSL measurements, S_{f+m} is normally used for dating because it would have been bleached in nature in a short time. However, S_{f+m} cannot be measured directly from the CW-OSL curve. In practice, S_{f+m} is estimated by subtracting an equivalent part at the end of the OSL curve from the initial part (Y_0). This is because the decay rate of the slow component is very slow and can be assumed to be constant during the measurement period (usually 40-100 s). Assuming that S_{f+m} , S_{s0} and B_0 have expectations μ_{f+m} , μ_s and μ_B , and variances σ_{f+m}^2 , σ_s^2 and σ_B^2 respectively, by extending Eqn. 1 in Galbraith's notation (Galbraith,

2002) to allow for the slow component, the variance of the estimate μ_{f+m} is written as

$$\text{Var}(\mu_{f+m}) = \sigma_{f+m}^2 + \sigma_s^2 + \sigma_B^2 + \frac{1}{k}\sigma_s^2 + \frac{1}{k}\sigma_B^2 \quad \text{Eqn. 2}$$

where k is the ratio of the number (m) of channels used for estimating μ_s and μ_B to the number (n) of channels used for estimating μ_{f+m} .

If S_{f+m} , S_{s0} and B_0 all follow a Poisson distribution, we have $\mu_{f+m} = \sigma_{f+m}^2$, $\mu_s = \sigma_s^2$, and $\mu_B = \sigma_B^2$, and this yields the same expression as equation 3 in Galbraith (2002),

$$\text{RSE}(\hat{\mu}_{f+m}) = \frac{\sqrt{Y_0 + \frac{1}{k}\bar{Y}}}{Y_0 - \bar{Y}} \quad \text{Eqn. 3}$$

where \bar{Y} is the average count per n channels in the last $k \cdot n$ channels, which is an estimate of $\mu_s + \mu_B$. This form is that generally used for error estimation of the background-corrected OSL.

However, if only S_{f+m} and S_{s0} have Poisson distributions, but B_0 does not, thus $\mu_{f+m} = \sigma_{f+m}^2$ and $\mu_s = \sigma_s^2$, but $\mu_B \neq \sigma_B^2$. Then Eqn. 2 becomes

$$\text{Var}(\mu_{f+m}) = \mu_{f+m} + (1 + \frac{1}{k})\mu_s + (1 + \frac{1}{k})\sigma_B^2 \quad \text{Eqn. 4}$$

which can be estimated as

$$\begin{aligned} \text{Var}(\hat{\mu}_{f+m}) &= Y_0 - \bar{Y} + (1 + \frac{1}{k})(\bar{Y} - \hat{\mu}_B) + (1 + \frac{1}{k})\hat{\sigma}_B^2 \\ &= Y_0 + \frac{1}{k}\bar{Y} + (1 + \frac{1}{k})(\hat{\sigma}_B^2 - \hat{\mu}_B) \end{aligned} \quad \text{Eqn. 5}$$

where $\hat{\sigma}_B^2$ and $\hat{\mu}_B$ are estimates of σ_B^2 and μ_B , respectively. Hence the RSE of $\hat{\mu}_{f+m}$ becomes

$$\text{RSE}(\hat{\mu}_{f+m}) = \frac{\sqrt{Y_0 + \frac{1}{k}\bar{Y} + (1 + \frac{1}{k})(\hat{\sigma}_B^2 - \hat{\mu}_B)}}{Y_0 - \bar{Y}} \quad \text{Eqn. 6}$$

Eqn. 6 is similar to equation 6 given in Galbraith (2002). However, in his note, the source of overdispersion is not directly known. It has been shown in the section above that the instrumental background is only dependent on the experimental conditions and

instruments, e.g. dark noise of instrument, thickness of filters and power of stimulation light. The values of $\hat{\mu}_B$ and $\hat{\sigma}_B^2$ can thus be obtained by multiplying the average values of the mean counts and variance shown in Table 1 by the channel number n used for obtaining Y_0 , providing that the same instrument and measurement conditions are used as those used in measuring annealed quartz with no OSL signal. Hence, the third term $(1 + \frac{1}{k})(\hat{\sigma}_B^2 - \hat{\mu}_B^2)$ in the numerator of Eqn. 6, the over-dispersion with respect to the Poisson variation in S_{F+m} , is expected to vary only slightly through all the measurements if the same experimental conditions and instruments are used and can be measured independently.

Dependence of background counts on signal intensity

An important assumption for calculating the background-subtracted OSL signal (as described in the previous section) is that the instrumental background should be independent of the measured signal (i.e. the background contribution of the PMT is the same no matter whether there is the presence of a signal or not). This is difficult/impossible to measure directly, but one possible experiment is to add a constant level of reflected light and look at the residuals around the average level. Such an experiment was carried out by reducing the thickness of the U340 filters from 7.5 mm to 2.5 mm to allow more scattered light to reach the PMT. Four blank discs were then measured four times by holding them at 125°C and using 0%, 10%, 30% and 50% of the maximum power of the blue LED stimulation system, respectively. This would result in different light intensities being measured. The observed mean photon count rate and the corresponding variance for each stimulation power are shown in Fig. 2a and b. As shown, the photon count rate increases linearly with the stimulation power (i.e. scattered light intensity). A similar trend was also observed for the variance, suggesting that the variance of the scattered light also increases with its intensity.

It can be expected that the counts for the scattered light should have a variance/mean ratio independent of its intensity, thus by subtracting the background observed when there is no stimulation light (power=0%) from the total signal with stimulation light (power>0%), the count rate from the scattered light and its variance can be estimated for different stimulation powers. If there is a dependence of background on the measured signal, subtracting the same background from the different signals observed at different stimulation powers would give different calculated variance/mean ratio for the scattered light.

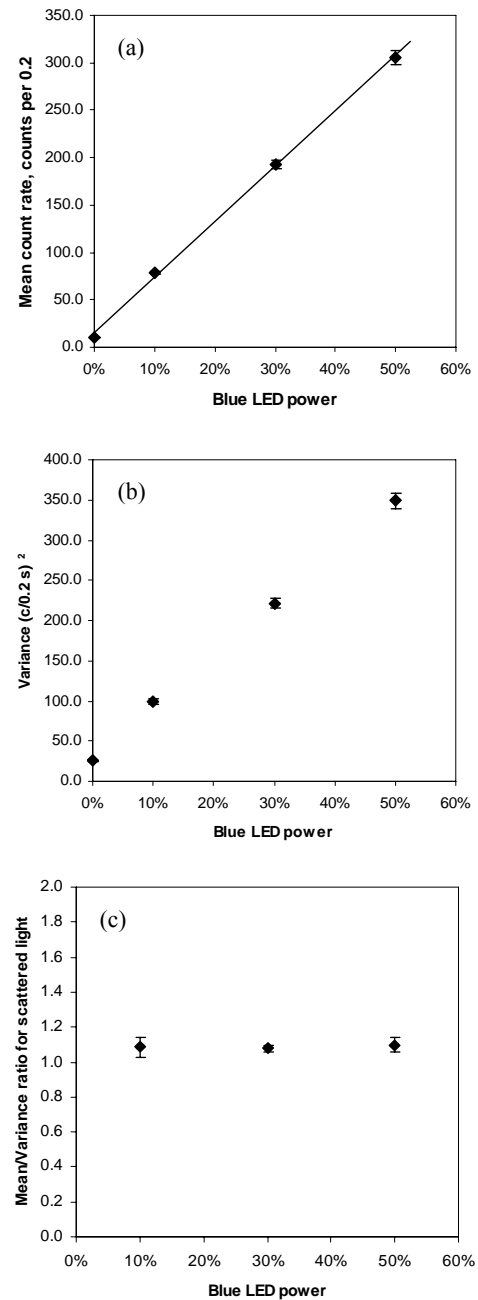


Figure 2: (a) The observed mean photon count rate plotted against the stimulation light power. (b) The variance for different stimulation powers. (c) The variance/mean ratio of the scattered light obtained by subtracting the background measured when there is no stimulation light.

On the other hand, if the same variance/mean ratio for the scattered light was obtained by subtracting the same background for different scattered light intensities, it suggests that the background is independent of signal level reaching the PMT. Fig. 2c

| Sample | Y_0 (cts/s) | \bar{Y} (cts/s) | RSE (%) | |
|--------|------------------|----------------------|------------|------------|
| | | | Equation 3 | Equation 6 |
| C5 | 209 | 153 | 27.5 | 36.4 |
| Wgs1 | 775 | 184 | 4.8 | 5.3 |
| TWC | 2201 | 148 | 2.29 | 2.35 |
| DGF-1 | 49061 | 1273 | 0.46 | 0.46 |

Table 2: Comparison of the relative standard error (RSE) of the background-corrected OSL signal from four different samples with different levels of OSL signal (see Fig. 3) calculated using Eqn. 3 and 6. Y_0 is the signal counts recorded in the first 1 second ($n=5$). \bar{Y} is calculated as the average of the signal counts observed in the last 5 seconds ($m=25$, $k=5$). The values of $\hat{\mu}_B$ and $\hat{\sigma}_B^2$ are 65 cts/s and 136 (cts/s)², respectively, which are estimated by multiplying the mean counts and variance in 0.2 s (Table 1) by the factor k .

shows the variance/mean ratio of the scattered light plotted as a function of the stimulation power. A similar ratio of ~ 1.1 was obtained for all stimulation powers used, suggesting that the background is independent of the measured signal. Therefore, one can use the background values obtained by measuring blank discs for calculating the error for the background-subtracted OSL signal as suggested in the previous section.

Effects of the non-Poisson distribution of instrumental background on error estimation

In order to investigate to what extent the nature of the instrumental background may influence the relative standard error (RSE) of the background-corrected OSL signal, typical OSL curves taken from four samples with different levels of OSL counts (Fig. 3) were analyzed using Eqn. 3 and 6, respectively. Y_0 is the signal counts recorded in the first 1 second ($n=5$).

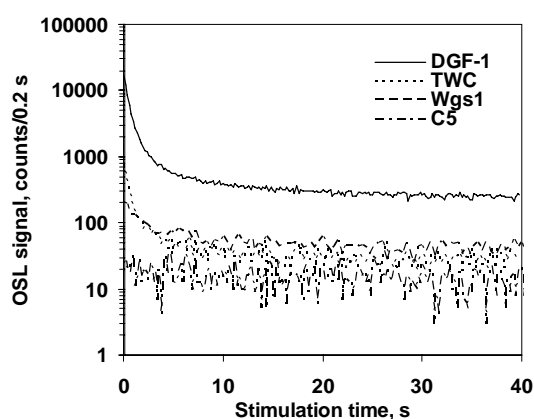


Figure 3: Typical OSL curves from four samples, C5, Wgs1, TWC and DGF-1, with different levels of OSL count rates. The OSL curves were measured at 125°C using blue LEDs with 50% of the maximum power.

\bar{Y} is calculated as the average of the signal counts observed in the last 5 seconds ($m=25$, $k=5$). The

values of $\hat{\mu}_B$ and $\hat{\sigma}_B^2$ are thus 5 times the average values obtained for 0.2 s (Table 1), i.e. $\hat{\mu}_B=13.0 \times 5=65$ and $\hat{\sigma}_B^2=27.2 \times 5=136$ (cts/s)² for $k=5$, respectively.

The value of RSE calculated using different methods are summarized in Table 2. For all samples the RSE values estimated from Eqn. 3 are smaller than those obtained using Eqn. 6. The difference between the RSE obtained from Eqn. 3 and that from Eqn. 6 is reduced as the total OSL counts increase. For the brightest sample DGF-1 (Fig. 3), the two values obtained from the two equations are indistinguishable from each other. This is expected because the contribution from $\hat{\sigma}_B^2$ to the total variance becomes smaller as the OSL signal increases. For the dimmest sample C5 (Fig. 3), the RSE of the background-corrected signal estimated from Eqn. 6 is 38.1%, significantly larger than the value of 27.5% given by Eqn. 3 when assuming that the background has a Poisson distribution.

Discussions

The results suggest that different relative contributions of the slow component and background may result in different counting distributions for the OSL signal and thus different extents of underestimation of the error, if Poisson distribution is simply assumed for all signals, i.e. the OSL signal and instrumental background. Therefore, Eqn. 3 can not be used for estimating the error for weak OSL signals because it may result in significant underestimation of the true error (up to 28% for the dimmest sample C5).

The implication of this result is especially important for young samples and single grains where the signal is relatively weak (e.g. Jain et al., 2004). For these applications, the RSE of the signal is very important for calculating the error in the age and interpreting

the age distribution using radial plots and different age models (e.g. Galbraith, 1990; Galbraith et al., 1999; Jacobs et al., 2006). If the RSE is poorly determined and subsequently used in a radial plot or in age models, e.g. the central age model, this may lead to misinterpretation of the distribution of the age population for the samples. Therefore, Eqn. 6 is recommended for the error estimation of OSL signals, especially those from young samples or dim samples; and this requires the values of $\hat{\mu}_B$ and its variance $\hat{\sigma}_B^2$ to be measured for each instrument. Although the author found that the values of $\hat{\mu}_B$ and $\hat{\sigma}_B^2$ vary negligibly over time, in practice, it is suggested that their values are checked once after every set of OSL measurements. It will be best to use similar discs with completely annealed quartz grains (e.g. annealed at 700°C for one hour) to duplicate the measurement conditions.

Conclusions

The counting distribution of the instrumental background in an OSL measurement is over-dispersed and does not follow a Poisson distribution. This may influence the error estimation of the background-corrected OSL signal substantially, especially for young samples with weak OSL signals.

Acknowledgements

The author thanks Dr. Sheng-hua Li, Prof. Ann Wintle, Prof. Geoff Duller, Dr. Richard Bailey and Prof. Rex Galbraith for their valuable comments.

References

- Bailey, R.M., Smith, B.W., Rhodes, E.J., 1997. Partial bleaching and the decay form characteristics of quartz OSL. *Radiation Measurements* **27**, 123-136.
- Banerjee, D., Bøtter-Jensen, L., Murray, A.S., 2000. Retrospective dosimetry: estimation of the dose to quartz using the single-aliquot regenerative-dose protocol. *Applied Radiation and Isotopes* **52**, 831-844.
- Bøtter-Jensen, L., Duller, G.A.T., Murray, A.S., Banerjee, D., 1999. Blue light emitting diodes for optical stimulation of quartz in retrospective dosimetry and dating. *Radiation Protection Dosimetry* **84**, 335-340.
- Galbraith, R.F., 1990. The radial plot: graphical assessment of spread in ages. *Nuclear Tracks and Radiation Measurements* **17**, 207-214.
- Galbraith, R.F., 2002. A note on the variance of a background corrected OSL count. *Ancient TL* **20**, 49-51.
- Galbraith, R.F., Roberts, R.G., Laslett, G.M., Yoshida H., Olley, J.M., 1999. Optical dating of single and multiple grains of quartz from Jinnium rock shelter, northern Australia: Part I, Experimental design and statistical models. *Archaeometry* **41**, 339-364.
- Jacobs, Z., Duller, G.A.T., Wintle, A.G., 2006. Interpretation of single grain D_e distributions and calculation of D_e . *Radiation Measurements* **41**, 264-277.
- Jain, M., Thomsen, K. J., Bøtter-Jensen, L., Murray, A. S., 2004. Thermal transfer and apparent-dose distributions in poorly bleached mortar samples: results from single grains and small aliquots of quartz. *Radiation Measurements* **38**, 101-109.
- Li, B., Li, S.H., 2006. Comparison of D_e estimation using the fast component and the medium component of the quartz OSL. *Radiation Measurements* **41**, 125-136.
- Smith, B.W., Rhodes, E.J., 1994. Charge movements in quartz and their relevance to optical dating. *Radiation Measurements* **23**, 329-333.

Reviewer

R.M. Bailey